IEEE Photonics Journal
An IEEE Photonics Society Publication

Open Access

Passive Q-Switching of a Diode-Pumped $Pr:LiYF_4$ Visible Laser Using WS_2 as Saturable Absorber

Volume 8, Number 3, June 2016

Yongjie Cheng
Jian Peng
Bin Xu
Han Yang
Zhengqian Luo
Huiying Xu
Zhiping Cai
Jian Weng

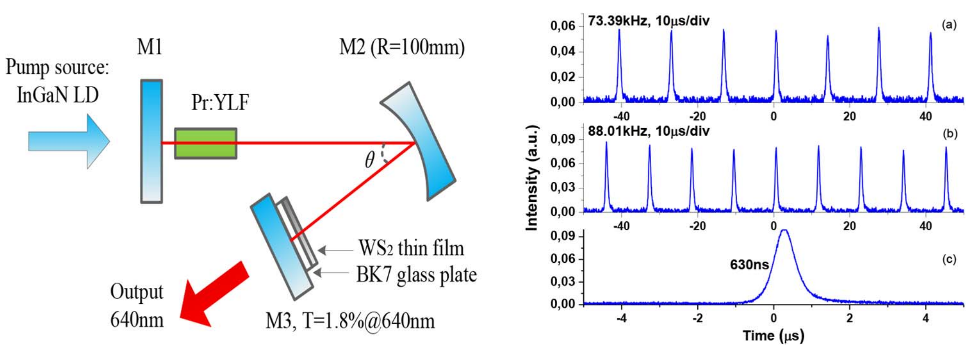

DOI: 10.1109/JPHOT.2016.2550804

Passive Q-Switching of a Diode-Pumped $Pr:LiYF_4$ Visible Laser Using WS_2 as Saturable Absorber

Yongjie Cheng,[1] Jian Peng,[2] Bin Xu,[1] Han Yang,[1] Zhengqian Luo,[1] Huiying Xu,[1] Zhiping Cai,[1] and Jian Weng[2]

[1]Department of Electronic Engineering, Xiamen University, Xiamen 361005, China
[2]Department of Biomaterials, Xiamen University, Xiamen 361005, China

DOI: 10.1109/JPHOT.2016.2550804

Manuscript received February 16, 2016; accepted March 31, 2016. Date of publication April 5, 2016; date of current version May 10, 2016. This work was supported in part by the National Natural Science Foundation of China under Grant 61275050, Grant 61475129, Grant 61575164; by the Specialized Research Fund for the Doctoral Program of Higher Education under Grant 20120121110034 and Grant 20130121120043; by the Fundamental Research Funds for the Central Universities under Grant 2013121022; by the Natural Science Foundation of Fujian Province of China under Grant 2014J01251; and by the Scientific Research Foundation for the Returned Overseas Chinese Scholars, State Education Ministry. Corresponding author: Z. Cai (e-mail: zpcai@xmu.edu.cn).

Abstract: Q-switched laser operation of a blue-diode-pumped $Pr:LiYF_4$ laser is demonstrated at 640 nm for the first time by using a tungsten disulfide (WS_2) nanosheet material as a saturable absorber. Stable laser pulses of 630 ns are obtained with a pulse repetition rate of 88 kHz, a pulse energy of about 0.24 μJ, and an average output power of 21.5 mW. This paper broadens the application of WS_2-like 2-D nanosheet saturable absorbers from the near- and mid-infrared to the visible domain.

Index Terms: Diode-pumped lasers, nonlinear effects in nanostructures, photon sources, Q-switched lasers, visible lasers.

1. Introduction

Passive Q-switching and mode-locking using various types of saturable absorbers have, for a long time, proven to be efficient techniques for the generation of high-peak power and short laser pulses with μs down to fs time durations. Among these saturable absorbers, Cr^{4+}:YAG crystal [1] and semiconductor saturable absorber mirrors (SESAMs) [2] have been probably the most popular ones in the past two decades because of their short recovery times and their ability to generate and support laser pulses with picosecond down to femtosecond time durations. However, the operating wavelengths of SESAMs are limited to particular spectral bands, and they require specific and expensive fabrication techniques. Moreover, except for a few examples [3], [4], most of these laser systems have been developed only for the near-infrared (NIR) and mid-infrared (MIR) wavelength domains.

During the last decade, however, other types of materials, such as carbon nanotubes (CNTs) [5] and graphene [6]–[8], have been found to be very promising as saturable absorbers in fiber- and other diode-pumped solid state lasers (DPSSLs). Therefore, efforts have been made to explore all these high-performance nanosheet materials because of their excellent properties, such as ultra-broadband saturable absorptions, low cost, and easy fabrication. This is the case

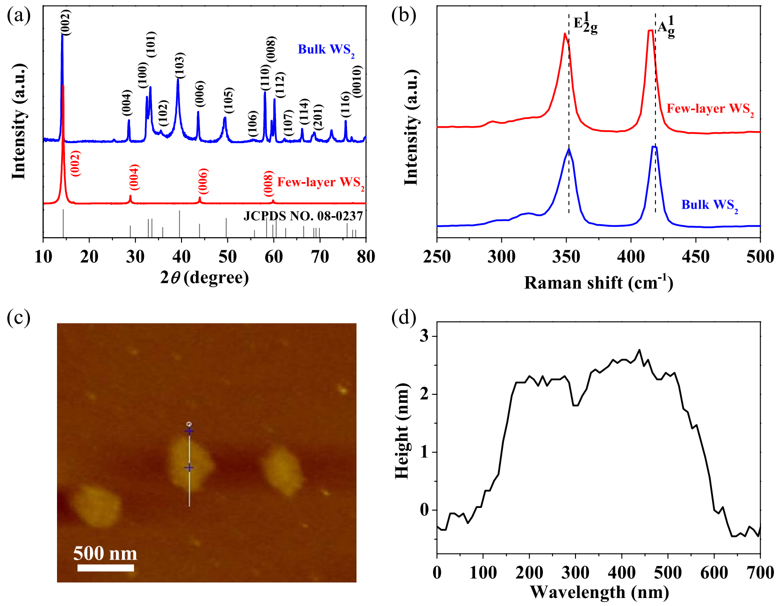

Fig. 1. (a) XRD pattern and (b) raman spectra, registered for bulk and few-layer WS_2. (c) AFM image and (d) height profile derived for the few-layers WS_2.

for new types of nanosheet materials, including Bi_2Se_3 [9]–[13], Bi_2Te_3 [14], and Sb_2Te_3 [15], which are grouped as topological insulators, as well as transition metal dichalcogenides like MoS_2 [16]–[18] and WS_2 [19], [20], all of them having already successfully worked as saturable absorbers in various types of lasers. However, at present, all these nanosheet materials have been only demonstrated again within NIR and MIR spectral domains. In 2012, a mode-locked Ti-sapphire laser at 800 nm based on monolayer graphene was demonstrated [21], which presents an important step towards nanosheet materials based visible pulsed laser. Further, very recently, visible pulsed lasers were also reported by using MoS_2 saturable absorber, which indicates that the few-layer sulfide could be the new promising material for visible pulsed laser generation [22]. However, exploiting such nanosheet saturable absorbers for passive Q-switching and mode-locking in the visible domain is still very challenging not only because of the difficulty to efficiently achieve visible laser source but also because of the predicament to produce nanosheet materials with suitable bandgap and good quality.

On the other hand, it is now well admitted that blue diode laser pumped visible lasers based on Pr^{3+} doped fluoride fibers and solid-state laser materials like ZBLAN and $LiYF_4$ offer the possibility of producing compact and efficient laser devices at many laser wavelengths from the blue to the deep-red [23]–[27]. Therefore, some nanosheet saturable absorbers able to operate this kind of visible lasers in the Q-switching or mode-locking regime would be much appreciated. In this letter, we show that it is possible to achieve passive Q-switching of a diode-pumped $Pr:LiYF_4$ laser operating at 640 nm by using a thin-film sample of WS_2 as a saturable absorber.

2. Preparation and Characterization of WS_2 SAs

The few-layer WS_2 used in our experiment was prepared by the liquid-phase exfoliation technique [28]. Initially, the purchased WS_2 (325 mesh power, alfa aesar) compound was added into the N-2-methylpyrrolidone (NMP) solution and sonicated for 20 hours to produce the few-layers WS_2 suspension. Purchased bulk WS_2 was characterized by X-ray diffraction [see XRD in Fig. 1(a)]. All the labeled peaks could be readily indexed to rhombohedral WS_2 (JCPDS no. 08-0237). The XRD pattern Fig. 1(a) of the few-layers WS_2 sample showed a high [002] orientation and some characteristic peaks disappeared compared to bulk WS_2, which indicates that

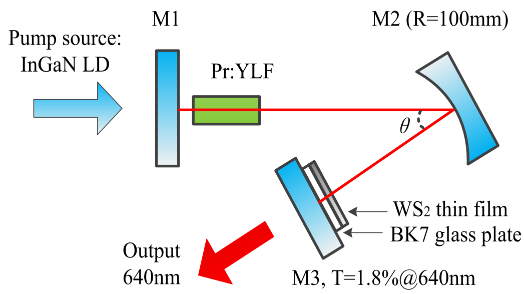

Fig. 2. Schematic experimental setup of the WS_2-based Q-switched Pr:YLF laser at 640 nm.

bulk WS_2 had been successfully exfoliated, as expected. As shown in Fig. 1(b), Raman spectroscopy was also used to characterize the WS_2 sample. The two peaks observed at 351 and 418 cm^{-1} are assigned to $E_{2g}{}^1$ and $A_g{}^1$ modes of the bulk WS_2. However, compared with the bulk WS_2, these peaks are slightly shifted to the red, which means some slight deviation of the lattice parameters. Furthermore, as shown in Fig. 1(c), the thickness of the as-prepared few-layers WS_2 was characterized by using atomic force microscopy (AFM). The average thickness [see Fig. 1(d)] derived from the height profile diagram was found equal to ~2–3 nm. Since the single-layer thickness is about 0.7 nm [28], it indicates that the WS_2 nano-sheets consisted of about three to four layers. The initial WS_2 solution was centrifuged first for 30 min at 2000 rpm to remove bulk WS_2. Subsequently, the supernatant was decanted to another centrifuge tube. After centrifugation of the supernatant at 13000 rpm for 30 min to remove free NMP, the as-obtained product was collected into phials for further application.

The WS_2 product was then transferred onto a BK7 glass substrate by using a commonly used spin-coating method and dried for 2 hours in an oven maintained at a temperature of 80 °C. The transmission of the as-prepared WS_2 saturable absorber was registered from 400 nm to 2700 nm (see Fig. 2). At the considered laser wavelength of 640 nm, the transmission was found equal to about 85.7%. The BK7 glass substrate has a transmission loss of about 8%, which means that the linear loss induced by the WS_2 thin film is about 6.3%. Using an open-aperture Z-scan technique, and a Ti:Sapphire pumped ~100 fs(with a 1 kHz repetition rate) optical parametric amplifier (OPA) operating at 635 nm, the modulation depth and saturable absorption intensity of the WS_2 were measured to be about 7.2% and 5.17 MW/cm^2, respectively. The experimental details on measuring the modulation depth and saturable absorption intensity have been reported separately [29].

3. Experimental Setup the WS_2-Based Q-Switched Pr:YLF Laser

The laser experimental setup is shown in Fig. 2. The pump source is a blue InGaN laser diode with an emitting wavelength of about 444 nm and a maximum output power of about 2 W. The laser diode was integrated with an aspheric lens (focal length $f = 3$ mm) for collimating the pump beam and then with a pair of cylindrical lenses ($f = 40$ and –8 mm) for correcting the astigmatism of the pump beam. After a 75-mm (focal length) focusing lens, the pump beam was injected into a 3×3 mm^2 cross section, 5-mm-long and 0.5at.% doped Pr:YLF crystal. The laser crystal was just wrapped inside an indium foil and mounted in a copper block without using any cooling device.

The laser resonator was a typical V-shaped three-mirror folded cavity. The flat input mirror M1 had a high transmission coating of 96.8% at the pump wavelength and a high reflection one of about 99.9% at the considered laser wavelength of 640 nm. The folded mirror M2 with a radius of curvature of 100 mm had a high reflection coating of 99.9% at 640 nm and a high transmission at the pump wavelength. The output mirror is also flat with a transmission of about 1.8% at 640 nm. The physical lengths between M1 and M2 as well as between M2 and M3 are about 128 mm and 69 mm, respectively. In order to reduce the astigmatism produced by the curved folded mirror M2, the folded angle θ was set to about 18%. For the Q-switched laser experiment,

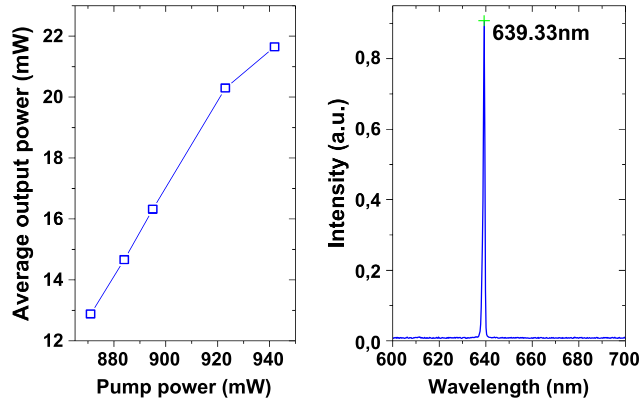

Fig. 3. (Left) Output power characteristics and (right) laser spectrum of the 640-nm Q-switched red laser.

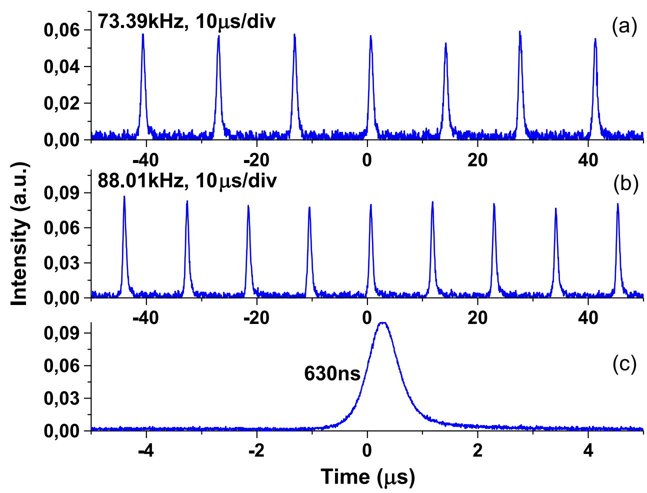

Fig. 4. Pulse trains obtained at pump power of (a) 870 and (b) 942 mW and (c) the shortest pulse profile.

the as-prepared WS_2 saturable absorber was inserted into the laser cavity very close to the output mirror. Note that such laser cavity avoids the influence of the residual pump laser on the WS_2 saturable absorber. The radius of the laser mode inside the WS_2 saturable absorber could be estimated to be about 35 μm.

4. Experimental Results and Discussions

Before inserting the saturable absorber inside the cavity, CW laser operation was obtained first with a pump threshold of about 350 mW and a maximum output power of about 156 mW. After inserting the WS_2 saturable absorber into the laser cavity, very close to the output mirror, pulsed laser operation was obtained at a pump threshold of about 700 mW but stable pulse trains and output peak powers were only obtained at a pump power exceeding about 870 mW. As shown in Figs. 3 and 4, above this pump power and up to about 920 mW, stable pulse trains could be obtained with an average output power increasing from about 12.5 mW to 21.5 mW. Above this pump level, Q-switching became again unstable, likely because of the non-optimized transfer quality of the WS_2 solution onto the glass substrate and of thermal load effects resulting from the poor thermal conductivity of this glass substrate.The pulse trains at threshold and maximum stable output and the shortest single pulse duration are shown in Fig. 5.

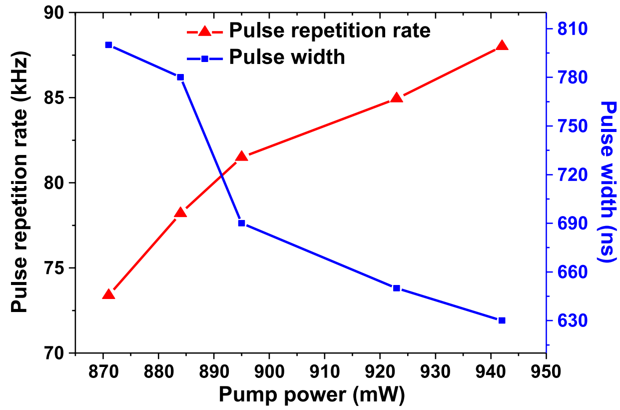

Fig. 5. Variations of pulse repetition rate and pulsewidth with pump power.

The evolutions of the pulse width and of the repetition with the absorbed pump power are reported in Fig. 5. From the stable Q-switching threshold to the maximum output power, the pulse width decreased from about 800 to 630 ns, while the pulse repetition rate increased from about 73.4 to 88 kHz, which means, for an average output power of 21.5 mW, pulse energies up to about 0.24 μJ.

5. Conclusion

In conclusion, we have demonstrated here for the first time that passive-Q-switching of a diode-pumped Pr:$LiYF_4$ laser operating around 640 nm was possible by using a solid-state nanosheet material made of a transition metal dichalcogenide WS_2 inside a simple V-shape laser cavity. Stable Q-switched laser operation with a maximum average output power of about 21.5 mW, laser pulses of about 630 ns time duration at a maximum pulse repetition rate of 88 kHz and single pulse energy of 0.25 μJ have been achieved. This can be compared with the 15 mW average output power (with 4 W incident pump power) and 0.18 nJ laser pulses obtained at a repetition rate of 85 MHz by mode-locking a Pr:$LiYF_4$ laser at 640 nm with a specially designed GaInP-quantum well-based SESAMs [3].

The present work paves the way for the development of ultra-compact diode-pumped pulsed laser devices in the visible domain. Works are in progress to improve the quality of the transfer of the material onto the substrate and by changing the substrate for another one with a better thermal conductivity.

Acknowledgment

The authors thank Prof. F. Wang, Nanjing University, for helping them to measure the modulation depth and saturable absorption intensity of their WS_2 sample.

References

[1] R. Abe, J. Kojou, K. Masuda, and F. Kannari, "Cr^{4+}-doped $Y_3Al_5O_{12}$ as a saturable absorber for a Q-switched and mode-locked 639-nm Pr^{3+}-doped $LiYF_4$ laser," *Appl. Phys. Exp.*, vol. 6, 2013, Art. no. 032703.

[2] U. Keller *et al.,* "Semiconductor saturable absorber mirrors (SESAM's) for femtosecond to nanosecond pulse generation in solid-state lasers," *IEEE J. Sel. Topic Quantum Electron.*, vol. 2, no. 3, pp. 435–453, Sep. 1996.

[3] M. Gaponenko *et al.,* "SESAM mode-locked red praseodymium laser," *Opt. Lett.*, vol. 39, no. 24, pp. 6939–6941, 2014.

[4] V. G. Savitski, I. M. Ranieri, A. B. Krysa, and S. Calvez, "Passively Q-switched Pr: YLF laser," in *Proc. IEEE CLEO*, 2011, pp. 1–2.

[5] A. Schmidt *et al.,* "Passive mode locking of Yb: KLuW using a single-walled carbon nanotube saturable absorber," *Opt. Lett.*, vol. 33, no. 7, pp. 729–731, 2008.

[6] Z. Q. Luo *et al.,* "Graphene-based passively Q-switched dual-wavelength erbium-doped fiber laser," *Opt. Lett.*, vol. 35, no. 21, pp. 3709–3711, 2010.

[7] W. D. Tan *et al.,* "Mode locking of ceramic Nd: Yttrium aluminum garnet with graphene as a saturable absorber," *Appl. Phys. Lett.*, vol. 96, no. 3, 2010, Art. no. 031106.

[8] J. L. Xu *et al.,* "Efficient graphene Q switching and mode locking of 1.34 μm neodymium lasers," *Opt. Lett.*, vol. 37, no. 13, pp. 2652–2654, 2012.

[9] Z. Q. Luo *et al.,* "1.06 μm Q-switched ytterbium-doped fiber laser using few-layer topological insulator Bi_2Se_3 as a saturable absorber," *Opt. Exp.*, vol. 21, no. 24, pp. 29516–29522, 2013.

[10] H. H. Yu *et al.,* "Topological insulator as an optical modulator for pulsed solid-state lasers," *Laser Photon. Rev.*, vol. 7, no. 6, pp. L77–L83, 2013.

[11] B. L. Wang *et al.,* "Topological insulator simultaneously Q-switched dual-wavelength Nd: Lu2O3 laser," *IEEE Photon. J.*, vol. 6, no. 3, Jun. 2014, Art. no. 1501007.

[12] C. J. Zhao *et al.,* "Wavelength-tunable picosecond soliton fiber laser with topological insulator: Bi_2Se_3 as a mode locker," *Opt. Exp.*, vol. 20, no. 25, pp. 27888–27895, 2012.

[13] B. Xu *et al.,* "Topological insulator Bi_2Se_3 based Q-switched Nd: $LiYF_4$ nanosecond laser at 1313 nm," *Opt. Exp.*, vol. 23, no. 6, pp. 7674–7680, 2015.

[14] P. H. Tang *et al.,* "Topological insulator: Bi_2Te_3 saturable absorber for the passive Q-switching operation of an in-band pumped 1645-nm Er: YAG ceramic laser," *IEEE Photon. J.*, vol. 5, no. 2, Apr. 2013, Art. no. 1500707.

[15] J. Sotor, G. Sobon, K. Grodecki, and K. M. Abramski, "Mode-locked erbium-doped fiber laser based on evanescent field interaction with Sb_2Te_3 topological insulator," *Appl. Phys. Lett.*, vol. 104, no. 25, 2014, Art. no. 251112.

[16] S. Wang *et al.,* "Broadband few-layer MoS_2 saturable absorbers," *Adv. Mater.*, vol. 26, no. 21, pp. 3538–3544, 2014.

[17] Z. Luo *et al.,* "1-, 1.5-, and 2-μm fiber lasers Q-switched by a broadband few-layer MoS_2 saturable absorber," *J. Light. Tech.*, vol. 32, no. 24, pp. 4679–4686, 2014.

[18] B. Xu *et al.,* "Passively Q-switched Nd: $YAlO_3$ nanosecond laser using MoS_2 as saturable absorber," *Opt. Exp.*, vol. 22, no. 23, pp. 28934–28940, 2014.

[19] D. Mao *et al.,* "WS_2 mode-locked ultrafast fiber laser," *Sci. Rep.*, vol. 5, 2015, Art. no. 07965.

[20] P. Yan *et al.,* "Microfiber-based WS_2-film saturable absorber for ultra-fast photonics," *Opt. Mater. Exp.*, vol. 5, no. 3, pp. 479–489, 2015.

[21] I. H. Baek *et al.,* "Efficient mode-locking of Sub-70-fs Ti: Sapphire laser by graphene saturable absorber," *Appl. Phys. Exp.*, vol. 5, 2012, Art. no. 032701.

[22] Y. Zhang *et al.,* "Atomic-layer molybdenum sulfide optical modulator for visible coherent light," *Sci. Rep.*, vol. 5, 2015, Art. no. 11342.

[23] B. Xu, P. Camy, J. L. Doualan, Z. Cai, and R. Moncorgé, "Visible laser operation of Pr^{3+}-doped fluoride crystals pumped by a 469 nm blue laser," *Opt. Exp.*, vol. 19, no. 2, pp. 1191–1197, 2011.

[24] A. Richter *et al.,* "Diode pumping of a continuous-wave Pr^{3+}-doped $LiYF_4$ laser," *Opt. Lett.*, vol. 29, no. 22, pp. 2638–2640, 2004.

[25] P. W. Metz *et al.,* "High-power red, orange, and green Pr^{3+}: $LiYF_4$ lasers," *Opt. Lett.*, vol. 39, no. 11, pp. 3193–3196, 2014.

[26] F. Reichert *et al.,* "Efficient laser operation of Pr^{3+}, Mg^{2+}: $SrAl_{12}O_{19}$," *Opt. Lett.*, vol. 37, no. 23, pp. 4889–4892, 2012.

[27] T. Gun, P. Metz, and G. Huber, "Power scaling of laser diode pumped Pr^{3+}: $LiYF_4$ cw lasers: Efficient laser operation at 522.6 nm, at 545.9 nm, 607.2 nm, and 639.5 nm," *Opt. Lett.*, vol. 36, no. 6, pp. 1002–1004, 2011.

[28] W. S. Yun *et al.,* "Thickness and strain effects on electronic structures of transition metal dichalcogenides: 2H-M X-2 semiconductors ($M = Mo$, W; $X = S$, Se, Te)," *Phys. Rev. B, Condens. Matter*, vol. 85, 2012, Art. no. 033305.

[29] Z. Q. Luo *et al.,* "Two-dimensional material-based saturable absorbers: Towards compact visible-wavelength all-fiber pulsed lasers," *Nanoscale*, vol. 8, pp. 1066–1072, 2016.